

## Optimisation of the control of Neoclassical Tearing Modes with ECCD in ASDEX Upgrade and ITER

M. Maraschek<sup>1</sup>, G. Gantenbein<sup>2</sup>, Q. Yu<sup>1</sup>, H. Zohm<sup>1</sup>, S. Günter<sup>1</sup>, F. Leuterer<sup>1</sup>, A. Manini<sup>1</sup>,  
ECRH group, ASDEX Upgrade Team<sup>1</sup>

<sup>1</sup>Max-Planck-Institut für Plasmaphysik, EURATOM Association, Garching, Germany

<sup>2</sup>Forschungszentrum Karlsruhe, Association EURATOM-FZK, IHM, D-76021 Karlsruhe, Germany

The ECCD deposition width during NTM stabilisation experiments has been scanned over a wide range relative to the island width. The highest efficiency in terms of stabilisation and achievable  $\beta_N$  with suppressed NTM could be achieved with a narrow deposition with the highest current density  $I_{ECCD}/d$ . For a broad deposition no stabilisation could be achieved. However, the NTM could be stabilised with modulated broad ECCD, depositing only in the islands O-point.

**Introduction** Neoclassical Tearing Modes (NTMs) are of great concern for tokamak plasmas, in particular for ITER and a future fusion reactor, as the presence of a (3/2)-NTM reduces the achievable  $\beta_N$  by at least 10-20%. As the achievable fusion power is proportional to  $\beta_N^2$  this is not tolerable.

Schemes for the stabilisation of NTMs by local co - Electron Cyclotron Current Drive (co-ECCD) with respect to the plasma current have been developed at various experiments [1–3] and established as a tool with feedback capabilities. Therefore in ITER a system with 24 MW ECCD power at 170 GHz has been foreseen for this purpose. Most of present experiments are performed with a fixed ECCD deposition width  $d$ , which is smaller than the marginal island size  $W_{marg}$ . For  $W < W_{marg}$  an NTM naturally decays away and  $\beta_N$  can rise again independently of the NTM size. For ITER, the condition  $d < W_{marg}$  is not necessarily fulfilled, and possible ways to reliably stabilise an NTM have to be developed for this purpose. The effect of the ratio  $d/W_{marg}$  has been investigated. The modulation of the ECCD depositing only power in the islands O-point is predicted to improve the efficiency of the stabilisation. This has been proved experimentally and is compared with predictions.

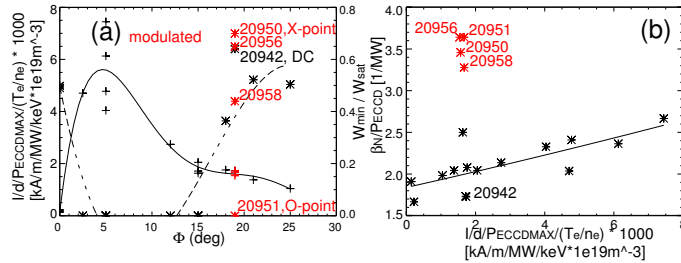


Figure 1: TORBEAM calculations of the width and total driven current. The ratio  $(I/d)/P_{ECCD}^{max}/(T_e/n_e)$  as function of the toroidal launching angle  $\Phi$  (plus signs, solid curve) is shown in (a) together with the experimentally achieved reduction of the (3/2)-NTM normalised to the island size without ECCD (stars, broken curve for unmodulated ECCD). (b) shows the achieved maximal  $\beta_N/P_{ECCD}$  as function of  $(I/d)/P_{ECCD}^{max}/(T_e/n_e)$ . In both figures the discharges with modulated ECCD are added in red.

The resonant surface is reached by a preprogrammed small scan of the magnetic field  $B_t \approx -2.0T \dots -2.3T$  towards higher absolute field. Based on TORBEAM calculations [4] the resulting deposition width  $d$ , current density  $j_{ECCD}$ , the total driven current  $I_{ECCD}$  and the resulting current peaking  $I_{ECCD}/d$  are calculated and shown in figure 1a. The current peaking is normalised to the maximal applied ECCD power  $P_{ECCD}^{max}$  and the ratio  $T_e/n_e$  in order to remove a variation in the driven current caused by different ECCD powers and different current drive efficiencies due to local plasma parameters.

From the calculations it can be seen that for a range  $\Phi \approx 2^\circ \dots 8^\circ$  the highest current density and hence

**Scan of the deposition width** The deposition width and the driven current of the ECCD mainly depend on the toroidal launching angle of the ECCD mirror ( $|\Phi| > 0^\circ$  for co-ECCD,  $\Phi = 0^\circ$  for pure heating). With the toroidal magnetic field  $B_t$  and the poloidal launching angle  $\Theta$  the major radius  $R_{dep}$  of the ECRH deposition and the resonant surface can be controlled, respectively. Only  $B_t$  can be varied during the discharge, whereas  $\Theta$  has to be fixed beforehand and at present can not be changed during the discharge at ASDEX Upgrade. Presently 3 gyrotrons with approximately 400kW each, with independent mirrors are available. Typically  $\Theta$  is adjusted in a way that the wave propagates through the plasma centre towards the deposition location on the high field

the highest  $I_{ECCD}/d$  are reached. Additionally the measured island size reduction  $W_{min}/W_{sat}(noECCD)$  is shown. For pure heating ( $\Phi = 0^\circ$ ) and broad deposition with low  $I_{ECCD}/d$  ( $\Phi \gtrsim 15^\circ$ ) no complete stabilisation with unmodulated ECCD, but only a reduction to typically half the saturated island size is achieved (figure 1a). Only in the range  $0^\circ > \Phi \gtrsim 15^\circ$  a complete stabilisation is possible.

Considering the achievable  $\beta_N$  for a given  $p_{ECCD}$  figure 1b (black points) shows  $\beta_N/P_{ECCD}$  as function of  $(I_{ECCD}/d)/P_{ECCD}^{max}/(T_e/n_e)$ . It can be clearly seen in the data points for unmodulated ECCD and in the corresponding linear fit, that with increasing current peaking  $(I_{ECCD}/d)/P_{ECCD}^{max}/(T_e/n_e)$  (current density  $j_{ECCD}$ ) the stabilisation gets more efficient and a higher  $\beta_N$  can be reached. The narrow deposition has been applied for the stabilisation of (3/2)-NTMs in improved H-mode discharges, where the NTM could be stabilised at the highest  $\beta_N \approx 2.5$  at the lowest  $q_{95} = 2.9$  at ASDEX Upgrade to date. This is below the ITER target value of  $q_{95} = 3.0$ .

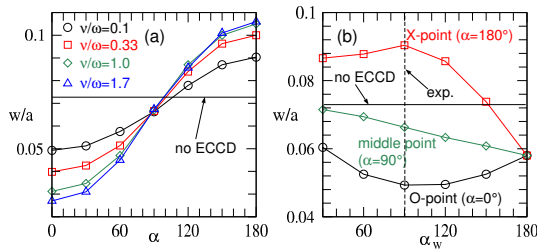


Figure 2: (a) Variation of the island size with modulated ECCD (50% duty cycle) for different phasings ( $\alpha = 0^\circ$  for O-point,  $\alpha = 180^\circ$  for X-point). The current drive efficiency is included by different normalised fast electron collisionalities  $\nu/\omega$  indicated with different colours and symbols. (b) For  $\alpha = 0^\circ, 90^\circ, 180^\circ$  a variation of the duty cycle from a short ECCD pulse ( $\alpha_w \rightarrow 0^\circ$ ) to continuous ECCD ( $\alpha_w = 180^\circ$ ) has been calculated. Experiments were performed with  $\alpha_w = 90^\circ$ .

ality is included, which governs the time it takes to build up the current in the O-point. Values of  $\nu \cdot \tau_R = 3 \cdot 10^3, 1 \cdot 10^4, 3 \cdot 10^4, 5 \cdot 10^4$  have been used, corresponding to  $\nu/\omega = 0.1, 0.33, 1.0, 1.7$ , with  $\omega$  representing the angular frequency of the mode and  $\tau_R = a^2 \mu_0 / \eta$  the resistive time scale. For  $\nu/\omega \ll 1$  it takes several tens of oscillations until the time averaged saturated ECCD current is reached. This is consistent with the increasing effect of the modulated ECCD with increasing  $\nu/\omega$  (figure 2a). For O and X-point phasing a stabilising and destabilising effects are predicted, respectively. A duty cycle of 50% is predicted to have the strongest effect for both phasings.

**Modulated ECCD with broad deposition** As shown above, with a broad ECCD deposition ( $\Phi > 15^\circ$ ) the NTM can not be stabilised completely and the achievable  $\beta_N/P_{ECCD}$  is reduced. By applying broad modulated ECCD with power deposition only in or near the islands O-point, a complete stabilisation can be regained (figure 3, #20951). A recovery to  $\beta_N = 2.0$  at  $q_{95} \approx 4.9$  could be achieved.

A direct comparison between 2 identical discharges clearly shows the improvement with O-point modulation (figure 3). In both cases the mode amplitude is initially reduced during the  $B_t$ -ramp when the ECCD moves radially into the island, but only in the modulated case the mode disappears and  $\beta_N$  recovers. In the unmodulated case  $\beta_N$  stays at values comparable to the time when the ECCD has not yet reached the resonant surface.

The data points for the modulated broad ECCD deposition are added in the diagrams in figure 1 in red. The current peaking is comparable to the unmodulated cases with  $\nu/\omega \geq 1$  assumed. The island size reduction for  $\Phi = 19^\circ$  shows a variation from complete stabilisation for #20951 to worse stabilisation than for the unmodulated case #20942 (see next section). The improvement in  $\beta_N/P_{ECCD}$  in figure

### Theoretical predictions for broad ECCD deposition

First theoretical considerations on the requirement of a modulation for NTM stabilisation assumed the deposition of the ECCD  $d$  to be smaller than the marginal island size  $W_{marg}$  [5]. With  $d/W_{marg} < 1$  modulation does not improve the efficiency of the ECCD significantly and has been no longer considered [1,5,6]. The case presented above has  $d/W_{marg} > 1$  and with the maximal ECCD power the (3/2)-NTM could be no longer stabilised. Calculations for  $d/W_{marg} > 1$  show, that the efficiency of ECCD stabilisation is significantly improved with modulation in the O-point of the island [6].

Calculations on the effect of the different phasings and duty cycles have been performed in order to gain a full understanding of the experimental findings. A deposition width of 20% of the minor plasma radius, i.e.  $d/a = 0.2$ , has been assumed. The phase angle  $\alpha$  and  $\alpha_w$  in figure 2 correspond to the phasing and the duty cycle of the ECCD, respectively. The considered model presently ignores the heating effect on the stabilisation efficiency [6]. The effect of the fast electron collision-

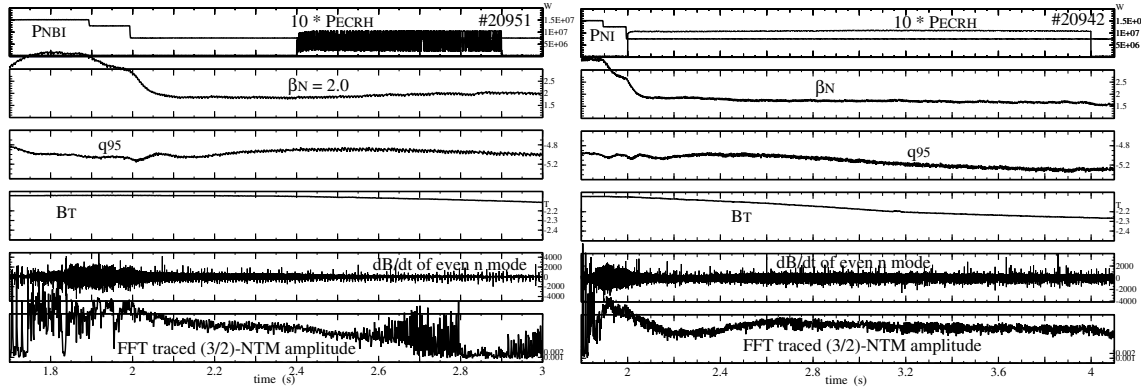


Figure 3: Stabilisation of a (3/2)-NTM in discharge #20951 with broad and modulated ECCD in the O-point of the island. The time traces show the heating power ( $P_{NBI}$  and the modulated  $P_{ECCD}$ ),  $\beta_N$ ,  $q_{95}$ , the preprogrammed ramped  $B_t$  for the resonance scan, the  $dB_{pol}/dt$  raw data and the FFT traced island amplitude of the (3/2)-NTM. A complete stabilisation can be observed after 2.7s. Discharge #20942 is identical, but unmodulated ECCD has been used, and the mode could not be stabilised.

1b shows two distinct groups for unmodulated and modulated discharges. For the unmodulated cases an improvement with increasing current peaking can be seen. For the modulated cases much higher values in  $\beta_N/P_{ECCD}$  can be observed. This is dominantly due to the halved average ECCD power to reach the same  $\beta_N$ . At present no deposition width scan has been performed for the modulated cases.

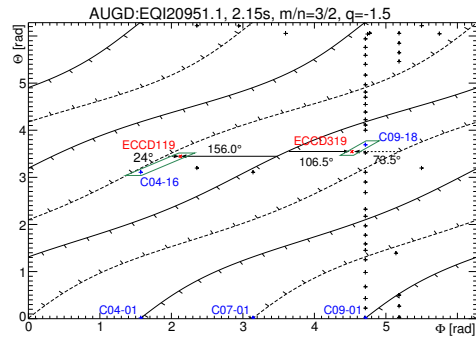


Figure 4: Mapping between the location of the ECCD deposition ( $\times$  signs) from TORBEAM calculations and the location of the Mirnov probes ( $+$  signs) considering the straight field line angle. The phase is adjusted to the location of the reference coils (C09-01 + C04-01). An additional phase check with the probes C04-16 and C09-18 for gyrotron 1 and 3,4, respectively, is possible.

**Effect of the phasing of modulated ECCD** In order to resolve the influence of the relative phase between the islands O-point and the deposited ECCD power, the ECCD has been modulated with different phases. The phase of the mode has been determined by a combination of Mirnov coils (measuring  $dB_{pol}/dt$ ). This phase has to be mapped along the magnetic field line on the  $q = m/n = 1.5$  resonant surface. One has to take the poloidally varying field line angle into account by using the so called straight field line angle  $\Theta^*(\Theta)$ . In the  $\Theta^*(\Theta) - \Phi$  plane field lines appear as straight lines and consequently the expected phase at the measurement positions can be reconstructed for arbitrary plasma shapes. In figure 4 the mapping between the reference coils and gyrotrons 1 and 3+4 is shown. For the modulation of the ECCD the sum of the signal of the two coils C09-01 and C04-01 has been used. They are located  $180^\circ$  toroidally apart. A precalculated phase shift for each gyrotron has been included taking into account the phase difference between the magnetic field line and the calculated ECCD deposition.

Based on the field line mapping the alignment of the ECCD deposition with the island can be compared with a subset of coils lying on the same magnetic field line as the ECCD deposition, as indicated in figure 5a (coil C04-16 for gyrotron 1 and coil C09-18 for gyrotrons 3 and 4). For both groups of gyrotrons and all coils the gyrotrons are injecting ECCD power mainly during the time interval with  $B_{pol}^{island} < 0$  ( $d(B_{pol}^{island}/dt)/dt > 0$ ). As the perturbation current within the island  $j_{island}$  flows parallel to the plasma current  $I_p$  in the X-point and antiparallel in the O-point, it becomes clear that the ECCD is deposited in phase with the islands O-point in discharge #20951 (figure 5a). The perturbation field  $B_{pol}^{island}$  has the same sign as the field from the plasma current  $B_{pol}^{plasma}$  at the X-point and the opposite sign at the O-point.

Consequently for the inverted phasing with deposition centred around the X-point of the island ( $B_{pol}^{island} > 0$ ) the smallest island size reduction is observed. In figure 1 discharge #20950 has the largest  $W_{min}/W_{sat}$ , i.e. the smallest island size reduction. Figure 5b shows the corresponding phasing close to the X-point. The remaining discharges were performed with modulated ECCD with different phasings between O and X-point corresponding to a variation of the angle  $\alpha$  in figure 2. As the two groups of gyrotrons do not have the same phasing and only an averaged phasing can be given, an experimental figure showing  $W_{min}/W_{sat}$  as function of  $\alpha_{experiment}$  can not be provided. A variation of the angle  $\alpha_w$  has experimentally not been performed.

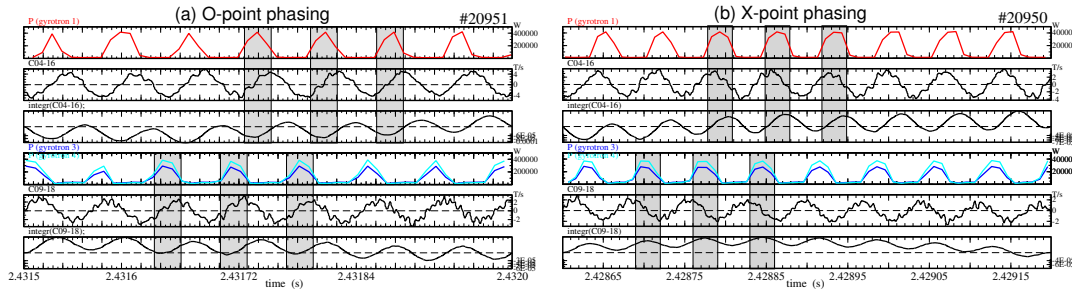


Figure 5: Zoom of the modulated ECCD power, the reference coils (C04-16,C09-18) and their integrated  $\frac{dB_{pol}^{island}}{dt}$  is shown. (a) Only for the O-point phasing of the ECCD in discharge #20951 the stabilisation for broad deposition could be recovered. The shaded times indicates the ECCD during the  $B_{pol}^{island} < 0$  phase for both gyrotron pairs. (b) For the inverted X-point phasing in discharge #20950 the smallest reduction of the island size has been observed. The shaded times indicate here  $B_{pol}^{island} > 0$  phase for both gyrotron pairs. Gyrotron 1 is not well aligned in this case.

**Stabilisation of (3/2)-FIR-NTMs at high  $\beta_N$**  The above discussed experiments have been performed in conventional ELMy H-modes after reducing the background NBI heating power in order to be able to stabilise the NTM with the installed ECCD power. The NTMs typically show a smooth behaviour in these cases, whereas at higher heating power and  $\beta_N > 2.3$  the (3/2)-NTM appears in the Frequently Interrupted Regime (FIR-NTM) [7,8]. In this high  $\beta_N$  scenario it is at present not possible to regain complete stabilisation with modulated broad ECCD deposition. However a clear reduction of the mode amplitude is observed with the modulation compared to the unmodulated case. The reduction does not appear in a smooth way, but with an enhanced drop of the island size at a naturally occurring FIR-drop when the ECCD depositing has reached the correct resonant surface.

**Summary and conclusions for ITER** A comprehensive scan of the (3/2)-NTM stabilisation efficiency on the deposition width of the ECCD has been performed. This clearly shows the advantage of a narrow deposition ( $d < W_{marg}$ ) and the loss of the stabilisation capability for broad deposition ( $d > W_{marg}$ ). With narrow deposition a significant improvement in terms of achievable  $\beta_N$  or a reduction of the required ECCD power to achieve a desired  $\beta_N$  has been observed.

It has been shown for the first time at ASDEX Upgrade that the loss of stabilisation for broad ECCD can be recovered by modulation of the ECCD with the phase of mode leading to a deposition in the islands O-point. Other phasings do not regain a stabilisation. This regain of stabilisation could also be partially observed at higher  $\beta_N$  with so-called FIR-NTMs.

## References

- [1] H. Zohm et al., Nucl. Fusion **39**, 577 (1999).
- [2] A. Isayama et al., Plasma Phys. Controlled Fusion **42**, L37 (2000).
- [3] R. J. La Haye et al., Phys. Plasmas **9**, 2051 (2002).
- [4] E. Poli, A. G. Peeters, and G. V. Pereverzev, Comput. Phys. Commun. **136**, 90 (2001).
- [5] G. Giruzzi et al., Nucl. Fusion **39**, 107 (1999).
- [6] Q. Yu, X. D. Yang, and S. Günter, Phys. Plasmas **11**, 1960 (2004).
- [7] S. Günter et al., Nucl. Fusion **43**, 161 (2003).
- [8] S. Günter et al., Nucl. Fusion **44**, 524 (2004).